Bulletin of Electrical Engineering and Informatics
Vol. 15, No. 6, December 2026, pp. 4745~4754
ISSN: 2302-9285, DOI: 10.11591/eei.v15i6.12256

Design, modeling, and control of standalone hybrid photovoltaic and wind energy conversion system

Lakshmi Dandapani[1], Manimegalai Subramanian[1,2], Malathy Batumalay[3], Taqwa Hariguna[4]
[1]Department of Electrical and Electronics Engineering, Faculty of Electrical and Electronic Engineering, AMET University, Chennai, India
[2]Department of Electrical and Electronics Engineering, Faculty of Electrical and Electronic Engineering, P.T. Lee Chengalvaraya Naicker College of Engineering and Technology, Kanchipuram, India
[3]Faculty of Data Science and Information Technology, INTI International University, Nilai, Malaysia
[4]Department of Computer Sciences, Amikom Purwokerto University, Purwokerto, Indonesia

Article Info

Article history:

Received Jan 6, 2026
Revised Aug 27, 2026
Accepted Sep 5, 2026

Keywords:

Adaptive neuro-fuzzy inference system
Doubly fed induction generator
Energy efficiency
High gain converter
Particle swarm optimization
Solar system
Wind energy conversion system

ABSTRACT

The growing demand for sustainable electricity generation has encouraged hybrid renewable energy systems that improve power availability and conversion efficiency under variable conditions. This study presents a hybrid photovoltaic (PV) and doubly fed induction generator (DFIG)-based wind energy conversion system (WECS) connected through a common direct current (DC) link. A high-gain DC–DC converter is employed in the PV subsystem and controlled using a hybrid particle swarm optimization (PSO) and adaptive neuro-fuzzy inference system (ANFIS) maximum power point tracking (MPPT) strategy. The complete system is modelled and evaluated in MATLAB/Simulink under irradiance variations of 700–1000 W/m² and constant wind speed of 8 m/s. The PSO–ANFIS controller achieves 96.18% tracking efficiency, while the converter reaches 94.7% conversion efficiency. These results demonstrate improved MPPT performance and voltage conversion, supporting the potential of the proposed architecture for hybrid PV–DFIG renewable energy systems.

This is an open access article under the CC BY-SA license.

Corresponding Author:

Malathy Batumalay
Faculty of Data Science and Information Technology, INTI International University
Nilai, Negeri Sembilan, Malaysia
Email: malathy.batumalay@newinti.edu.my

1. INTRODUCTION

The increasing global demand for energy has intensified concerns regarding energy security, environmental sustainability, and the long-term availability of conventional resources [1]–[3]. Renewable energy has therefore become an important alternative to fossil-fuel-based generation. Among renewable technologies, photovoltaic (PV) and wind energy conversion systems (WECS) are widely adopted for sustainable electricity generation [4]–[9]. However, PV generation depends on solar irradiance and temperature, while wind generation varies with wind speed and direction. Integrating PV and WECS in a hybrid configuration can complement these characteristics and improve the continuity and reliability of renewable power generation [10]–[12].

Effective coordination of PV and wind subsystems remains challenging because maximum power extraction must be maintained under changing environmental conditions. A doubly fed induction generator (DFIG) is suitable for variable-speed wind operation because its rotor-side converter enables controlled power exchange over a range of speeds. In the PV subsystem, maximum power point tracking (MPPT) is required to maintain operation near the maximum power point, while the direct current-direct current (DC–DC) converter

adapts the PV voltage to the required DC-link level. Conventional boost converters may require high duty ratios for large voltage gains, increasing semiconductor stress and power losses. Therefore, high-gain converter topologies are attractive for improving voltage conversion performance in hybrid renewable-energy systems.

MPPT performance directly affects PV energy extraction efficiency. Conventional and optimization-based techniques may experience oscillations, slow convergence, or reduced tracking accuracy under rapidly changing conditions [13]–[15]. Intelligent control methods have consequently been investigated to improve MPPT performance [16], [17]. However, achieving fast convergence, accurate tracking, and stable operation simultaneously remains challenging [18]. Adaptive neuro-fuzzy inference system (ANFIS) provides adaptive nonlinear modelling and control capabilities, but its performance depends on appropriate parameter selection and training [19]. Particle swarm optimization (PSO) can provide an effective optimization mechanism for parameter adjustment, while ANFIS can perform adaptive nonlinear mapping. Their combination therefore offers complementary optimization and learning capabilities.

Previous studies have demonstrated the potential of intelligent and hybrid control methods for renewable-energy conversion systems [20]–[22]. However, further investigation is required on the integration of a PSO–ANFIS MPPT controller with a high-gain DC–DC converter and DFIG-based WECS within a coordinated hybrid PV–wind architecture. Such integration can provide a common DC-link structure in which the PV and wind subsystems operate through their respective conversion stages before supplying the alternating current (AC) load. The performance of the proposed system should therefore be assessed in terms of MPPT tracking, voltage regulation, and power-conversion efficiency under changing operating conditions.

To address this gap, this study proposes a hybrid PV–DFIG renewable-energy system incorporating a high-gain DC–DC converter and PSO–ANFIS MPPT controller. The proposed controller combines PSO-based parameter optimization with the adaptive nonlinear learning capability of ANFIS to improve PV maximum power tracking under varying irradiance. The proposed converter provides high voltage gain for DC-link integration, while the DFIG-based WECS complements the PV subsystem. The system is modelled and evaluated in MATLAB/Simulink under varying irradiance and wind conditions. Comparative analysis is performed against perturb and observe (P&O), PSO, and ANFIS MPPT methods and against conventional boost, single-ended primary-inductor converter (SEPIC), and modified boost converters. The evaluation focuses on MPPT tracking efficiency, DC-link voltage, AC output performance, and converter efficiency, providing a basis for further development toward real-time implementation, energy storage, and smart-grid applications.

2. METHOD

The proposed hybrid renewable energy system integrates a PV array, a variable-speed WECS based on a DFIG, a high-gain DC–DC converter, a hybrid PSO–ANFIS MPPT controller, a three-phase AC–DC rectifier, a DC-link capacitor, and a single-phase DC–AC inverter. The overall configuration is shown in Figure 1. In the PV path, the measured PV voltage and current are processed by the PSO–ANFIS controller to generate the duty-ratio pulse width modulation (PWM) signal for the high-gain converter. The converter increases the PV voltage and transfers the extracted power to the common DC link. In the wind path, the DFIG output is converted through the AC–DC stage and supplied to the same DC link. The DC-link capacitor combines and stabilizes the power from both renewable sources before the inverter supplies the AC output. This common-DC-link configuration enables coordinated power conversion from the PV and wind subsystems [23], [24].

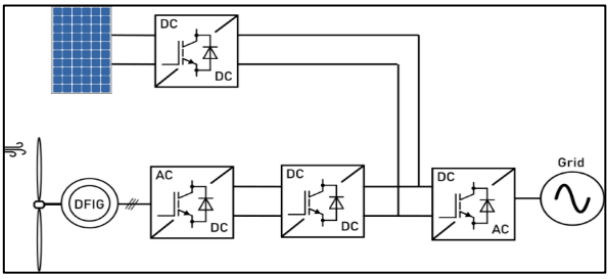


Figure 1. A schematic representation of the proposed study

2.1. Photovoltaic system and high-gain converter

The PV subsystem converts solar irradiance into electrical power through an array of series- and parallel-connected solar cells [22], [25]. The equivalent PV cell model consists of a photocurrent source, diode, and series and parallel resistances, as illustrated in Figure 2. The cell current is expressed as (1):

$$\left[I = I_L - I_{SC}\left[\exp\left(\frac{q(U+IR_S)}{AKT}\right) - 1\right] - \frac{U+IR_S}{R_P}\right] \quad (1)$$

where (I_L) is the photocurrent, (I_{SC}) is the reverse saturation current, (q) is the electron charge, (K) is the Boltzmann constant, (T) is the cell temperature, (A) is the diode factor, and (R_S) and (R_P) are the series and parallel resistances.

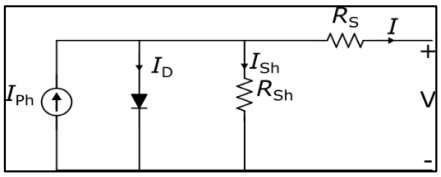


Figure 2. Equivalent circuit of a solar cell

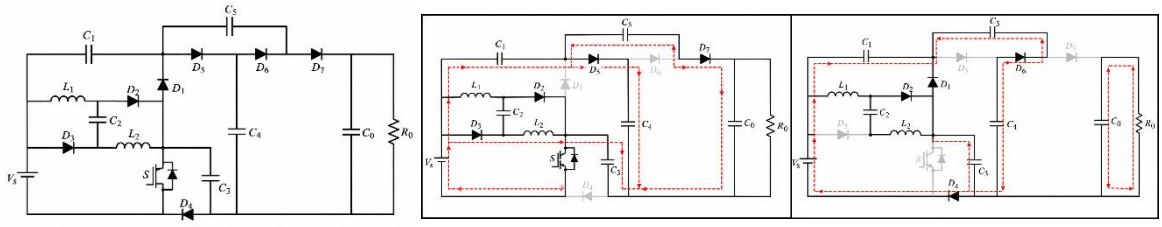
The proposed high-gain DC–DC converter, shown in Figure 3, provides the interface between the PV array and the common DC link. The complete figure presents the converter topology and its two main switching modes [26]. As shown in Figure 3(a), the proposed topology consists of one active switch, two inductors, seven diodes, and six capacitors. Switched-capacitor and voltage-lift cells are employed to achieve high voltage gain at a relatively low duty ratio. The converter operates in two main switching modes, with the ON and OFF states illustrated in Figures 3(b) and (c), respectively. The principal voltage relationships for each switching state are derived using Kirchhoff's voltage law (KVL) and Kirchhoff's current law (KCL) [27], [28]. The resulting voltage gain is expressed as (2):

$$\left[\frac{V_{Out}}{V_S} = \frac{6}{1-D}\right] \quad (2)$$

where (D) is the duty ratio. The corresponding current relationship is given by (3):

$$\left[I_{Out} = \frac{6}{1-D} I_S\right] \quad (3)$$

The switching waveforms of the proposed converter are presented in Figure 4, showing the switching signal and the corresponding inductor, diode, and source/output responses.



(a) (b) (c)

Figure 3. High-gain converter; (a) equivalent circuit, (b) mode 1, and (c) mode 2

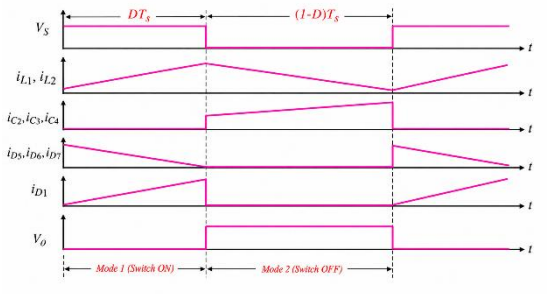


Figure 4. Switching waveforms of the high-gain converter

2.2. Hybrid PSO–ANFIS MPPT controller

The hybrid PSO–ANFIS controller is used to determine the maximum power operating point of the PV array under changing irradiance. ANFIS provides nonlinear mapping and adaptive learning, while PSO optimizes the ANFIS parameters to improve the tracking response [29]–[32]. The ANFIS structure consists of five layers that process the input variables and generate the control output, as shown in Figure 5. The controller uses the measured PV voltage and current as inputs and generates the converter duty ratio as the control output.

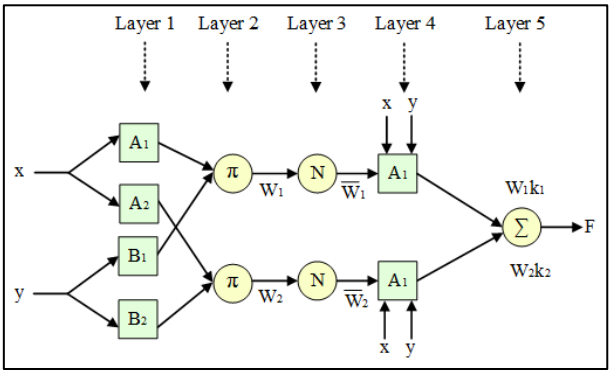


Figure 5. Structure of the ANFIS controller

The ANFIS output is determined from the weighted membership functions and consequent parameters, while the training error is evaluated using the root mean square error (RMSE). PSO iteratively adjusts the ANFIS parameters until the predefined convergence criterion is satisfied. The resulting optimized model generates the PWM duty ratio for the high-gain converter. The overall training and control procedure is illustrated in Figure 6. The proposed control scheme therefore establishes a closed-loop relationship between the PV operating conditions and the high-gain converter. Changes in PV voltage and current are processed by the optimized ANFIS model to continuously adjust the converter duty ratio and maintain operation near the maximum power point under varying irradiance.

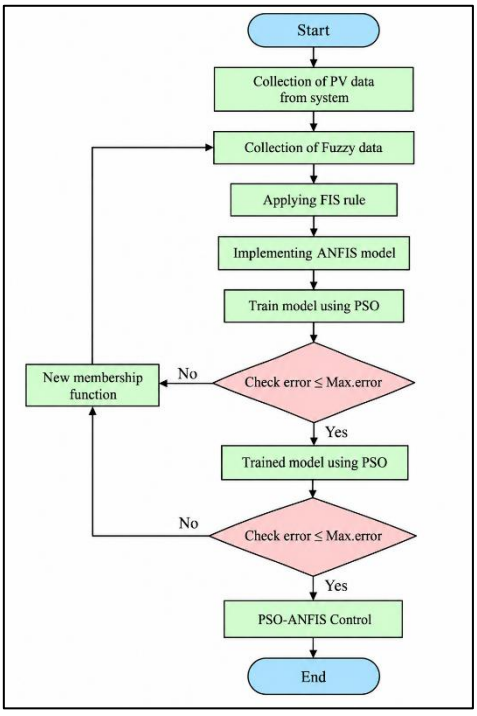


Figure 6. Flowchart of the hybrid PSO–ANFIS MPPT algorithm

2.3. Doubly-fed induction generator-based wind energy conversion system and inverter

The wind subsystem employs a DFIG with three-phase stator and rotor windings connected through slip rings. The DFIG enables variable-speed operation through controlled rotor current. Using the (dq) reference-frame transformation, the dynamic voltage equations are expressed as (4) [9]:

$$\left.\begin{aligned} v_{ds} &= r_s i_{ds} + \frac{d\psi_{ds}}{dt} - \omega_s \psi_{qs} \\ v_{qs} &= r_s i_{qs} + \frac{d\psi_{qs}}{dt} + \omega_s \psi_{ds} \\ v_{dr} &= r_r i_{dr} + \frac{d\psi_{dr}}{dt} - \omega_r \psi_{qr} \\ v_{qr} &= r_r i_{qr} + \frac{d\psi_{qr}}{dt} + \omega_r \psi_{dr} \end{aligned}\right\} \quad (4)$$

where (r_s) and (r_r) are the stator and rotor resistances, and (ω_s) and (ω_r) are the synchronous and rotor angular speeds. The corresponding flux linkages are given by (5):

$$\left.\begin{aligned} \psi_{ds} &= L_s i_{ds} + L_m i_{dr} \\ \psi_{qs} &= L_s i_{qs} + L_m i_{qr} \\ \psi_{dr} &= L_r i_{dr} + L_m i_{ds} \\ \psi_{qr} &= L_r i_{qr} + L_m i_{dqs} \end{aligned}\right\} \quad (5)$$

where (L_s), (L_r), and (L_m) denote the stator, rotor, and mutual inductances, respectively. The electromagnetic torque is expressed as (6):

$$T_{em} = P\left(\psi_{ds} I_{ds} - \psi_{qs} I_{ds}\right) \quad (6)$$

where (P) is the number of pole pairs. The stator active and reactive powers are calculated as (7):

$$\left.\begin{aligned} P_s &= \frac{3}{2}\left(v_{ds} i_{ds} + v_{qs} i_{qs}\right) \\ Q_s &= \frac{3}{2}\left(v_{qs} i_{ds} - v_{ds} i_{qs}\right) \end{aligned}\right\} \quad (7)$$

The DC-link voltage is converted into AC power using the single-phase full-bridge inverter shown in Figure 7. The inverter consists of four switches operated alternately in complementary pairs to generate the required AC output. The DC-link capacitor provides an intermediate interface between the PV and wind conversion stages and helps maintain a stable DC voltage. The inverter subsequently delivers the combined renewable power to the grid.

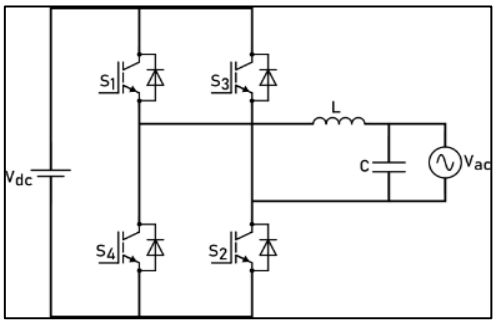


Figure 7. Single-phase inverter

Overall, the proposed system combines PV and DFIG-based wind generation through a common DC link. The PV subsystem employs the PSO–ANFIS MPPT controller and high-gain DC–DC converter, while the wind subsystem uses the DFIG and AC–DC conversion stage. The combined DC power is regulated through the DC-link capacitor and converted to AC by the single-phase inverter.

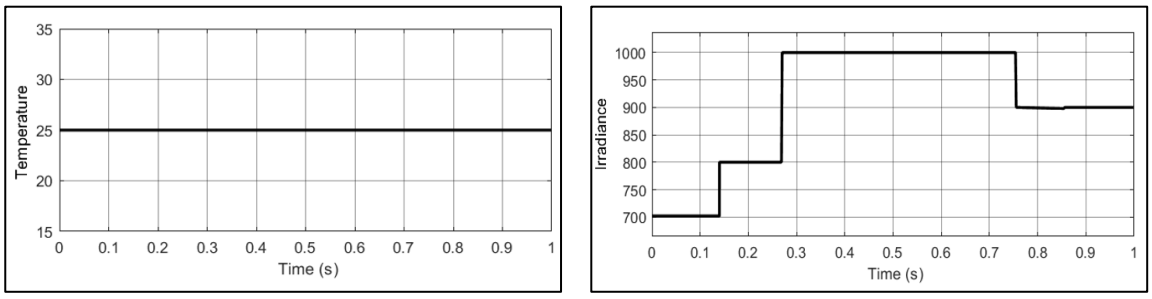
3. RESULTS AND DISCUSSION

The proposed hybrid PV–DFIG system was simulated using MATLAB/Simulink under variable solar irradiance and constant wind speed. The PV irradiance was varied from 700 to 1000 W/m², while the wind speed was maintained at 8 m/s. The PV array consisted of 15 modules, each rated at 100 W, with an open-circuit voltage of 22.67 V, short-circuit current of 5.87 A, maximum power voltage of 18.76 V, and maximum power current of 5.41 A, as summarized in Table 1.

Table 1. Specifications of solar panel

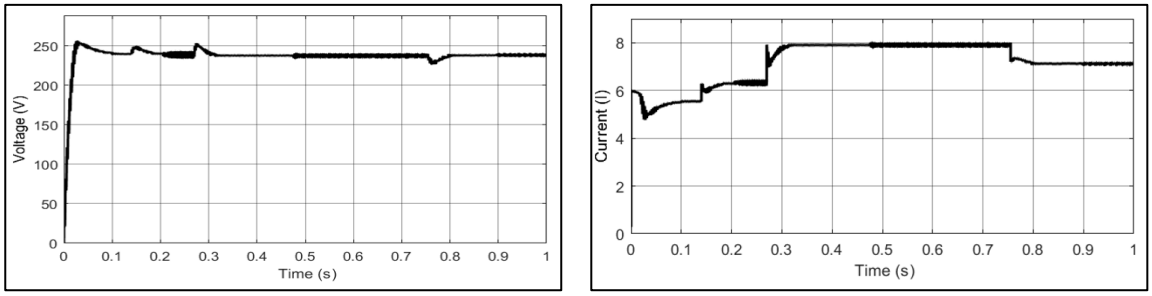
Parameters	Value
Maximum power (P_{mp})	100 W
Number of modules in a PV array	15
Open circuit voltage (V_{oc})	22.67 V
Short circuit current (I_{sc})	5.87 A
Maximum voltage (V_{mp})	18.76 V
Maximum current (I_{mp})	5.41 A
Number of cells in series (N_s)	36

The temperature was maintained at 25 °C, while the irradiance was varied stepwise from 700 to 1000 W/m², as shown in Figure 8. Figure 8(a) illustrates the variation in solar irradiance, which initially increased from 700 W/m² to 800 W/m² and subsequently to 1000 W/m² before decreasing to approximately 900 W/m². Figure 8(b) presents the corresponding temperature profile, which remained constant at 25 °C throughout the test. The corresponding PV voltage and current responses are presented in Figure 9. Figure 9(a) shows the PV voltage response, which reached approximately 243 V at 700 W/m² and increased slightly to around 250 V at higher irradiance levels. Figure 9(b) presents the PV current response, which increased from approximately 5.61 A to 8 A as the irradiance increased. The relatively stable voltage and responsive current indicate that the proposed PSO–ANFIS controller maintained the PV operating point under changing irradiance. At a constant wind speed of 8 m/s, the DFIG-based WECS generated electrical power and supplied it to the common DC link, as shown in Figure 10. Figure 10(a) presents the DFIG voltage response, while Figure 10(b) shows the corresponding current response. These responses demonstrate the electrical behavior of the DFIG-based WECS under the specified operating condition.



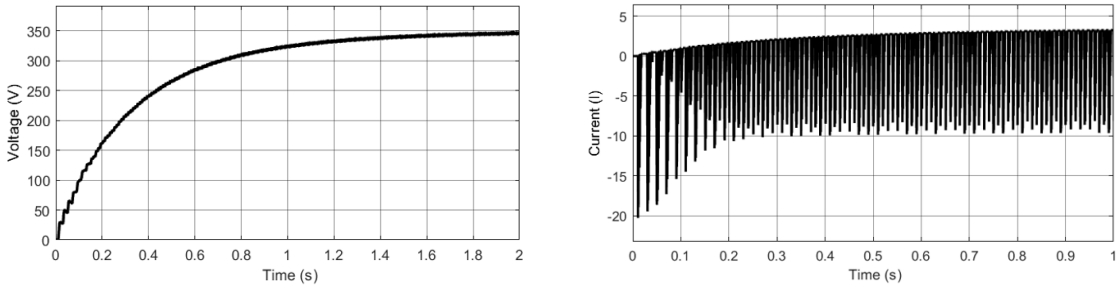
(a) (b)

Figure 8. Solar PV system operating conditions; (a) temperature and (b) irradiance



(a) (b)

Figure 9. Output of PV fed proposed converter; (a) voltage and (b) current



(a) (b)

Figure 10. DFIG-based WECS electrical responses; (a) voltage and (b) current

The stator voltage increased gradually and reached approximately 350 V after 1.5 s, while the current exhibited a sinusoidal response with transient oscillations during the initial operation. The combined renewable power was then transferred through the DC link. As shown in Figure 11, the DC-link voltage increased from 0 V to approximately 530 V within 0.1 s and remained relatively stable during the simulation. The regulated DC-link voltage was converted into AC using the single-phase voltage-source inverter. The output waveforms are shown in Figure 12, where the inverter produced an approximately sinusoidal voltage with a peak value of ±520 V and current of approximately ±2 A. The voltage and current were in phase, indicating a resistive load condition and stable inverter operation.

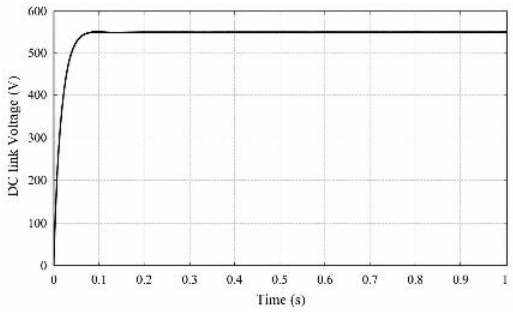


Figure 11. DC link voltage

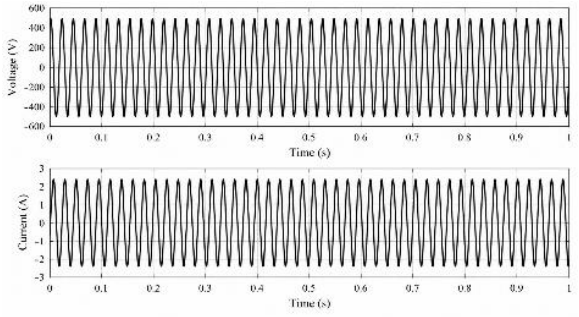


Figure 12. AC output waveform

The proposed PSO–ANFIS MPPT controller was compared with P&O, PSO-based, and ANFIS-based methods, as shown in Figure 13. The P&O, PSO, and ANFIS methods achieved approximately 89%, 91%, and 93% tracking efficiency, respectively, whereas the proposed PSO–ANFIS controller achieved 96.18%. The improved performance is attributed to the combination of PSO-based parameter optimization and ANFIS adaptive nonlinear mapping. The proposed high-gain converter was also compared with conventional boost, SEPIC, and modified boost converters in Figure 14. Their efficiencies were approximately 88%, 91%, and 92%, respectively, while the proposed converter achieved 94.7%.

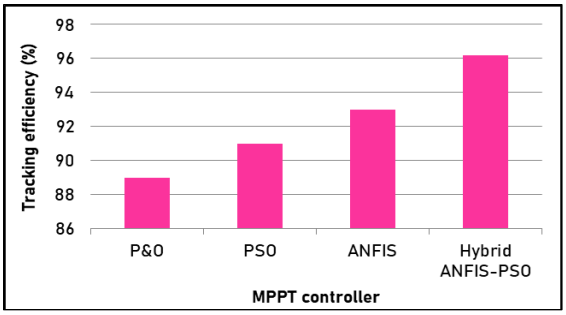


Figure 13. Comparative study on tracking efficiency

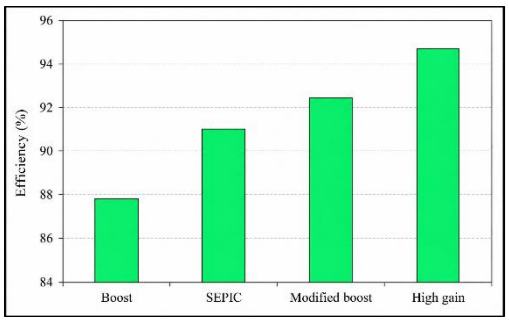


Figure 14. Efficiency comparison of converters

Overall, the simulation results demonstrate that the proposed PSO–ANFIS MPPT controller and high-gain converter provide improved tracking and conversion efficiency under the investigated operating conditions. The hybrid system maintained a stable DC-link voltage and produced a sinusoidal AC output while integrating PV and DFIG-based wind power. However, these results are based on MATLAB/Simulink simulations and should be further validated through experimental implementation and broader operating conditions.

4. CONCLUSION

This study presented the design, modelling, and performance evaluation of a hybrid PV and DFIG-based WECS integrated through a common DC link with a hybrid PSO–ANFIS MPPT controller and high-gain DC–DC converter. The proposed PSO–ANFIS controller achieved a tracking efficiency of 96.18%, outperforming the P&O, PSO-based, and ANFIS-based methods, while the proposed high-gain converter achieved 94.7% efficiency, exceeding the conventional boost, SEPIC, and modified boost converters. Under PV irradiance of 700–1000 W/m², a temperature of 25 °C, and wind speed of 8 m/s, the system maintained stable operation, with the DC-link voltage reaching approximately 530 V and the inverter producing a stable AC output. These results demonstrate that the coordinated PSO–ANFIS controller and high-gain converter can improve power extraction and voltage conversion in hybrid PV–DFIG systems. However, the validation was limited to MATLAB/Simulink simulations under fixed wind speed and temperature. Future work should investigate wider environmental and load conditions, partial shading, real-time and hardware-in-the-loop implementation, grid-connected operation, battery energy storage, and scalability to larger hybrid renewable-energy systems.

FUNDING INFORMATION

Authors state no funding involved.

AUTHOR CONTRIBUTIONS STATEMENT

This journal uses the Contributor Roles Taxonomy (CRediT) to recognize individual author contributions, reduce authorship disputes, and facilitate collaboration.

Name of Author	C	M	So	Va	Fo	I	R	D	O	E	Vi	Su	P	Fu
Lakshmi Dandapani	✓	✓	✓	✓	✓	✓		✓	✓	✓				✓
Manimegalai		✓				✓		✓	✓	✓	✓	✓		
Subramanian														
Malathy Batumalay	✓		✓	✓			✓			✓	✓		✓	✓
Taqwa Hariguna				✓		✓			✓		✓			✓

C : **C**onceptualization
M : **M**ethodology
So : **So**ftware
Va : **Va**lidation
Fo : **Fo**rmal analysis
I : **I**nvestigation
R : **R**esources
D : **D**ata Curation
O : Writing - **O**riginal Draft
E : Writing - Review & **E**diting
Vi : **Vi**sualization
Su : **Su**pervision
P : **P**roject administration
Fu : **Fu**nding acquisition

CONFLICT OF INTEREST STATEMENT

Authors state no conflict of interest.

DATA AVAILABILITY

The data that support the findings of this study are available from the corresponding author, MB, upon reasonable request.

REFERENCES

[1] J. V. Antony and A. A. K., "MPPT Integrated High Gain DC-DC Converter for PV-fed Three Phase Induction Motor Drive," in *RAICS - IEEE Recent Advances in Intelligent Computational Systems*, 2024, doi: 10.1109/RAICS61201.2024.10689848.
[2] A. M. Elkhatat and S. Al-Muhtaseb, "Climate change and energy security: A comparative analysis of the role of energy policies in advancing environmental sustainability," *Energies*, vol. 17, 2024, p. 3179, doi: 10.3390/en17133179.
[3] Z. Yu, J.-F. Mao, and Y.-T. Li, "Dynamic links between economic complexity, technological innovation, structural transformation

and energy sustainability in newly industrializing countries," *Scientific Reports*, vol. 15, 2025, doi: 10.1038/s41598-025-24685-2.
[4] R. Kumar and M. V. Naik, "Solar PV Array Fed Zeta Converter- VSI Controlled BLDC Motor Drive for Water Pumping System," in *2024 IEEE Students Conference on Engineering and Systems (SCES)*, IEEE, Jun. 2024, pp. 1–6, doi: 10.1109/SCES61914.2024.10652421.
[5] D. A. Dewi and T. B. Kurniawan, "Analyzing the Impact of Social Media and Influencer Endorsements on Game Revenue using Multiple Linear Regression in the Metaverse," *International Journal Research on Metaverse*, vol. 2, no. 2, pp. 167–182, Jun. 2025, doi: 10.47738/ijrm.v2i2.29.
[6] K. Başaran, F. Bozyiğit, P. Siano, and D. Kılınç, "Systematic literature review of photovoltaic output power forecasting," *IET Renewable Power Generation*, 2020, doi: 10.1049/iet-rpg.2020.0351.
[7] V. Saxena, N. Kumar, B. Singh, and B. K. Panigrahi, "Wind-PV Based Microgrid Assisted EV Charging Infrastructure Control," in *2022 IEEE International Conference on Power Electronics, Drives and Energy Systems (PEDES)*, IEEE, Dec. 2022, pp. 1–5, doi: 10.1109/PEDES56012.2022.10080263.
[8] R. J. Rashes, "Adaptive blockchain-orchestrated supply chain resilience through predictive maritime disruption intelligence," *Journal of Current Research in Blockchain*, vol. 3, no. 3, pp. 200–215, 2026, doi: 10.47738/jcrb.v3i3.80.
[9] S. A. Khan, M. M. H. Chowdhury, and U. Nandy, "Solar-wind-power hybrid power generation system," *Journal of Engineering Research and Reports*, vol. 25, no. 10, 2023, p. 1007, doi: 10.9734/jerr/2023/v25i101007.
[10] N. H. Saad and A. Zekry, "Enhancing the energy utilization of hybrid renewable energy systems," *International Journal of Renewable Energy Research*, vol. 10, no. 4, 2020, doi: 10.20508/ijrer.v10i4.11537.g8098.
[11] Z. Bouguerra and A. Benfdila, "Modelling and Simulation of PV/WECs Hybrid System Controlled by Fuzzy Logic Control," in *2023 1st International Conference on Renewable Solutions for Ecosystems: Towards a Sustainable Energy Transition (ICRSEtoSET)*, IEEE, May 2023, pp. 1–5, doi: 10.1109/ICRSEtoSET56772.2023.10525669.
[12] A. Couto and A. Estanqueiro, "Wind power plants hybridised with solar power: A generation forecast perspective," *Journal of Cleaner Production*, 2023, p. 138793, doi: 10.1016/j.jclepro.2023.138793.
[13] M. N. S. Khairi, N. A. B. Bakhari, A. A. A. Samat, N. Kamarudin, M. H. Md Hussin, and A. I. Tajudin, "MPPT Design Using PSO Technique for Photovoltaic System," in *2023 IEEE 3rd International Conference in Power Engineering Applications (ICPEA)*, IEEE, Mar. 2023, pp. 131–136, doi: 10.1109/ICPEA56918.2023.10093161.
[14] M. L. Katche, A. B. Makokha, S. O. Zachary, and M. S. Adaramola, "A comprehensive review of maximum power point tracking (MPPT) techniques used in solar PV systems," *Energies*, vol. 16, 2023, p. 2206, doi: 10.3390/en16052206.
[15] M. Bakare, A. Abdulkarim, A. Shuaibu, and M. M. Mustafa, "Enhancing solar power efficiency with hybrid GEP ANFIS MPPT under dynamic weather conditions," *Scientific Reports*, vol. 15, 2025, doi: 10.1038/s41598-025-90417-1.
[16] S. Bachikh, Z. Abdellah, A. Necaibia, A. Seghiour, and I. Barbaui, "Contribution to the MPPT control strategy for a photovoltaic system: a comparative study of PO, INC, and PSO," in *2023 Second International Conference on Energy Transition and Security (ICETS)*, Adrar, Algeria, Dec. 2023, pp. 1–6, doi: 10.1109/ICETS60996.2023.10410797.
[17] B. Amirkhanov *et al.*, "Enhancing Sustainable Biogas Generation Through a Real-Time Digital Twin of a Modular Bioreactor," *Journal of Applied Data Sciences*, vol. 6, no. 4, pp. 2312–2331, Dec. 2025, doi: 10.47738/jads.v6i4.779.
[18] M. Abdelsattar, H. Mohamed, and A. Z. Z. Diab, "Maximum power point tracking of photovoltaic module based on Particle Swarm Optimization enhanced with Quasi-Newton method," *PLOS ONE*, vol. 20, 2025, p. e0327542, doi: 10.1371/journal.pone.0327542.
[19] P. Boonraksa, P. Peerapong, K. Palachai, P. Chotipintu, T. Boonraksa, and B. Marungsri, "An Evaluation of ANFIS Controller for Photovoltaic MPPT using Zeta Converter," in *Proceeding - 12th International Electrical Engineering Congress: Smart Factory and Intelligent Technology for Tomorrow, iEECON 2024*, Pattaya, Thailand, Mar. 2024, pp. 1–4, doi: 10.1109/iEECON60677.2024.10537943.
[20] D. Fortuna and C. J. Hutagalung, "Uncovering Lifestyle and Mental Well-being Predictors of Academic Performance Change in Online Learning: A Comparative Analysis of Interpretable Machine Learning Models," *Artificial Intelligence in Learning*, vol. 1, no. 4, pp. 271–286, Dec. 2025, doi: 10.63913/ail.v1i4.10.
[21] N. Priyadarshi, S. Padmanaban, J. Holm-Nielsen, F. Blaabjerg, and M. Bhaskar, "An experimental estimation of hybrid ANFIS–PSO-based MPPT for PV grid integration under fluctuating sun irradiance," *IEEE Systems Journal*, vol. 14, pp. 1218–1229, 2020, doi: 10.1109/JSYST.2019.2949083.
[22] N. Jittratorn, C. S. Liu, C. M. Huang, and H. T. Yang, "PV Power Forecasting for Operation of BESS Integrated with a PV Generation Plant," in *2024 IEEE 19th Conference on Industrial Electronics and Applications, ICIEA 2024*, IEEE, Aug. 2024, pp. 1–6, doi: 10.1109/ICIEA61579.2024.10664871.
[23] S. Singh and H. Bansal, "Hardware-in-loop implementation of an adaptive MPPT controlled PV-assisted EV charging system with vehicle-to-grid integration," *Scientific Reports*, vol. 15, 2025, doi: 10.1038/s41598-025-12508-3.
[24] H. A. Hussain, J. Loncarski, L. B. Ristic, and A. Bellini, "DFIG-Based WECS with Partial-Scale Converter: Efficiency, Cost, and Volume Comparison of SiC-Based and IGBT-Based Converter Solution," *IEEE Access*, vol. 12, pp. 89908–89920, 2024, doi: 10.1109/ACCESS.2024.3419810.
[25] N. C. Ramadani and S. Fahreza, "Quantifying the Dominant Role of Channel Audience in Predicting YouTube Success with Machine Learning," *Journal of Digital Society*, vol. 1, no. 4, pp. 258–271, 2025, doi: 10.63913/jds.v1i4.10.
[26] Z. Liu, Z. Liu, R. Dian, and H. Ouyang, "Parameter Identification and Extended State Observer-Based Predictive Control for Single-Phase Inverter," in *Proceedings of the 35th Chinese Control and Decision Conference, CCDC 2023*, Yichang, China, May 2023, pp. 1313–1318, doi: 10.1109/CCDC58219.2023.10327116.
[27] T. P. Singh, "SSD-based PSPWM inverter control for grid-integrated PV/wind system with EPO-based MPPT using high gain converter," *Electric Power Components and Systems*, vol. 52, pp. 2609–2623, 2023, doi: 10.1080/15325008.2023.2275716
[28] N. B. Dao, B. Dogan, S. Ghosh, E. Kazemzadeh, and M. Radulescu, "Toward sustainable ecology: how do environmental technologies, green financial policies, energy uncertainties, and natural resources rents matter?," *Clean Technologies and Environmental Policy*, vol. 27, no. 3, pp. 1387–1405, Mar. 2025, doi: 10.1007/s10098-024-02887-y.
[29] M. Aldulaimi and M. Çevik, "AI-enhanced MPPT control for grid-connected photovoltaic systems using ANFIS-PSO optimization," *Electronics*, vol. 14, 2025, p. 2649, doi: 10.3390/electronics14132649.
[30] M. S. Hasibuan, R. Z. A. Aziz, D. A. Dewi, T. B. Kurniawan, and N. A. Syafira, "Recommendation Model for Learning Material Using the Felder Silverman Learning Style Approach," *HighTech and Innovation Journal*, vol. 4, no. 4, pp. 811–820, Dec. 2023, doi: 10.28991/HIJ-2023-04-04-010.
[31] D. Lakshmi, C. N. Ravi, R. Zahira, S. Palanisamy, and S. Chenniappan, "Introduction to renewable energy sources and bulk power system," in *Power Systems Operation with 100% Renewable Energy Sources*, Elsevier, 2024, pp. 1–13, doi: 10.1016/B978-0-443-15578-9.00008-X.
[32] I. A. Ja'e *et al.*, "Assessment of thermo-mechanical performance of lightweight fibre-reinforced LECA concrete for enhanced energy efficiency," *Case Studies in Thermal Engineering*, vol. 71, pp. 1–19, 2025, doi: 10.1016/j.csite.2025.106189.

BIOGRAPHIES OF AUTHORS



Lakshmi Dandapani is a senior member of IEEE and a professor in the Department of Electrical and Electronics Engineering at AMET, Chennai, India. She received her B.E. from the University of Madras, M.E. from Anna University, and Ph.D. from Anna University. With over 25 years of teaching and research experience, she has supervised numerous undergraduate, postgraduate, and research scholars. She has authored 9 books, 22 book chapters, and over 85 journal papers, along with nearly 60 conference papers. She holds international, design, and utility patents and has received several awards for teaching and research. Her research interests include power systems, power quality, renewable energy, microgrids, load frequency control, and artificial intelligence in smart grids. She can be contacted at email: lakshmiee@gmail.com.



Manimegalai Subramanian is currently pursuing her Ph.D. (part-time) at AMET University, Chennai-603102, India. She is an assistant professor in the Department of Electrical and Electronic Engineering at P.T. Lee Chengalvaraya Naicker College of Engineering and Technology, Kanchipuram, India. Her research focuses on enhancing power quality in microgrids and modelling/designing hybrid energy systems. She can be contacted at email: manimegalais@ptleecncet.com.



Malathy Batumalay is a professor at the Faculty of Data Science and Information Technology, INTI International University, Malaysia. She holds a Ph.D. in Photonics from the University of Malaya and has extensive research and teaching experience in optical fiber and photonics. Her research interests include photonics, optical fiber sensing, nanomaterial-based sensors, and fiber optic devices. She has authored and co-authored numerous international journal and conference publications on fiber optic sensors and advanced photonic structures. She can be contacted at email: malathy.batumalay@newinti.edu.my.



Taqwa Hariguna is a researcher and professor of computer science at Universitas Amikom Purwokerto, Indonesia. He holds a Ph.D. from Southern Taiwan University of Science and Technology. His research interests include e-government, information systems, technology acceptance, software engineering, and digital transformation. He has published extensively in Scopus-indexed international journals and conferences, focusing on user behavior, service quality, and technology adoption. He can be contacted at email: taqwa@amikompurwokerto.ac.id.